An efficient numerical study for anisotropic nonlinear models of competitive swimming species

GEORGES CHAMOUN
Faculty of engineering (ESIB)
Saint Joseph University of Beirut
B.P 11-514 Riad El Solh, Beyrouth 1107 2050
LEBANON

Abstract: Traditional mathematical modeling and computational efforts have primarily focused on isotropic and linear diffusion or convection of living organisms, assuming uniform motion in all directions. However, these traditional models fail to capture the complexities of the real world where competitive interactions among species in nature often involve spatially heterogeneous and anisotropic diffusive behaviors. Another challenging aspect of such modeling involves scenarios in fluid dynamics, where species' movements are influenced by the flow of the medium. Besides the well-posedness of the mathematical model, this paper is also devoted to investigate an efficient and robust combined finite volume-nonconforming finite element scheme for two-species chemotaxis-fluid models including all layers of complex geometrical configurations. Moreover, numerous simulations through a developed code, cover the anisotropic dynamics of species in fluids which ensures the scheme's applicability to real-world biological problems. Furthermore, the training data generated through this flexible generalized numerical method may be enhanced with artificial intelligence techniques to improve the predictive capabilities.

Key-Words: Chemotaxis-fluid models, Anisotropic tensors, Degenerate coefficients, Global existence, Finite Volume method (FV), Finite Element method (FE), Interspecies competition.

Received: March 11, 2024. Revised: August 9, 2024. Accepted: September 10, 2024. Available online: October 21, 2024.

1 Introduction

The exploration of biological mechanisms through mathematical and numerical analysis has significantly advanced over the past decade. This shift has transformed any experimental science into a predictive one through computational simulations. Before presenting our comprehensive model that incorporates all potential constraints, it is essential to review the relevant literature. One of the basic models is the predator-prey system, initially introduced by Lotka in [1] and further developed by Volterra in [2]. These models describe the dynamics of two interacting species through a set of ordinary differential equations (ODEs):

$$\begin{cases} \dot{M} &= \mu_1 M(1 - M - \alpha_1 W) \\ \dot{W} &= \mu_2 W(1 - W - \alpha_2 M). \end{cases} \quad (1)$$

In this system, M and W represent the populations of the predator and prey, respectively. The parameters μ_1 and μ_2 are the growth rates, while α_1 and α_2 denote the interaction coefficients between the species. System (1) has four critical points $O(0,0)$, $N_1(1,0)$, $N_2(0,1)$ and $N_3(\frac{1-\alpha_1}{1-\alpha_1\alpha_2}, \frac{1-\alpha_2}{1-\alpha_1\alpha_2})$. The solutions of the system (1) exhibit different behaviors depending on the values of α_1 and α_2. In the weak competition regime, where α_1, $\alpha_2 \in (0,1)$, the solutions converge to the stable node N_3 that represents a coexistence equilibrium. In contrast, in the strong competition regime, where $0 < \alpha_1 < 1 < \alpha_2$ or $0 < \alpha_2 < 1 < \alpha_1$, the solutions tend towards the stable nodes N_1 or N_2, indicating the dominance of one species over the other. For more results on related competitive systems, the reader may refer to [3] and [4].

The dynamics of various populations is also based on the species' capacity to orient their movement in response to chemical gradients. This attraction or repulsion is called chemotactic motion. For a single species, the most classical model of chemotaxis was introduced by Keller and Segel in [5], and it has been extensively studied in [6] and recently in weighted networks in [7]. To simulate complex behaviors such as prey evasion or predator pursuit, the Lotka-Volterra species competition and chemotactic effects were combined in [8]. Extensive research has also been conducted on coupling chemotaxis effects with SIR-type equations to investigate the spatial spread of pandemics (see [9]). Further inquiry into the persistence of competitive exclusion, incorporating chemotaxis and competitive interactions between two species, can be found in the relevant literature [10, 11].

This paper is devoted to the numerical analysis of the following system including all these

complex scenarios in fluid environments,

$$\begin{cases} \partial_t M - \nabla \cdot \Big(Q(x)\big(a(M)\nabla M - \chi_1(M)\nabla C\big)\Big) \\ +U \cdot \nabla M = \mu_1 M(1 - M - \alpha_1 W), \\ \\ \partial_t W - \nabla \cdot \Big(R(x)\big(b(W)\nabla W - \chi_2(W)\nabla C\big)\Big) \\ +U \cdot \nabla W = \mu_2 W(1 - W - \alpha_2 M), \\ \\ \partial_t C - \nabla \cdot (S(x)\nabla C) + U \cdot \nabla C \\ = -(\alpha M + \beta W)C, \\ \\ \partial_t U - \nu\Delta U + \kappa(U \cdot \nabla)U + \nabla P \\ = -(\gamma M + \lambda W)\nabla\phi, \\ \\ \nabla \cdot U = 0, \text{ in } \Omega\times]0,T], \end{cases} \tag{2}$$

where Ω is an open bounded domain in $\mathbb{R}^d$ $(d \leq 4)$ with smooth boundary $\partial\Omega$. The system is supplemented by the following boundary conditions on $\partial\Omega \times (0,T)$,

$$Q(x)a(M)\nabla M \cdot \eta = 0, R(x)b(W)\nabla W \cdot \eta = 0, \tag{3}$$
$$S(x)\nabla C \cdot \eta = 0, U = 0,$$

where η is the exterior unit normal to $\partial\Omega$. The initial conditions on Ω are given by,

$$M(x,0) = M_0(x), W(x,0) = W_0(x), \tag{4}$$
$$C(x,0) = C_0(x),\ U(x,0) = U_0(x)\,.$$

The details, regarding all the variables of the system (2), are provided in the Table 1.

This model incorporates the dynamics of the fluid through the Navier-Stokes equations, or alternatively by the Stokes equations when the parameter κ equals zero. The diffusion equations exhibit a "volume-filling" biological condition, which prevents the overcrowding of the species. This effect is achieved through the diffusion coefficients $a(M)$ and $b(W)$, which approach zero as the population densities M and W approach a certain threshold.

This threshold represents the environment's carrying capacity, and in normalized form, it is set to 1. A common example of a diffusion-density coefficient is $a(M) = M(1 - M)$ for $M \in [0,1]$, reflecting natural constraints on movement. The chemotactic sensitivity, denoted as χ_1 or χ_2, indicates whether the species are attracted to or repelled from the chemical signals. A positive sign signifies attraction, while a negative sign indicates repulsion. In our model, the fluid is coupled to the chemotaxis equations through both

Table 1: Variables description

Variables	**Description**
M, W	The density of species 1 and 2
C	The concentration of the chemical
U, P	The velocity and the pressure of the fluid
Q, R **and** S	The anisotropic diffusive tensors
$a(M)$, $b(W)$	The density-dependent diffusion coefficients
$\chi_1(M)$, $\chi_2(W)$	The chemotactic sensitivity functions
μ_1, $\mu_2 > 0$	The growth rate of populations 1 and 2
α_1, $\alpha_2 > 0$	The strength of populations 1 and 2 in competition
α, $\beta > 0$	The consumption rate of chemicals by populations 1 and 2
$-(\gamma M + \lambda W)\nabla\phi$	The external gravitational force exerted by the species 1 and 2 on the fluid

the transport of species and chemical substrates $U \cdot \nabla M$, $U \cdot \nabla M$, $U \cdot \nabla C$. Additionally, the system incorporates the effect of an external gravitational force g acting along the upwards unit vector $\vec{z}$.

First, the question of the global existence of weak solutions of the model (2) has been well investigated and hence our system is well-posed. Recently, subsequent research has established the asymptotic dynamics for the two-species linear isotropic chemotaxis-fluid equations under sufficient conditions in 2D and 3D (see [12] and [13]).

Next, this paper aims to study the system (2) numerically. Unfortunately, the most results in the literature are for systems with linear non-degenerate isotropic diffusion in a fluid at rest (see [14]). Additionally, this paper presents a developed numerical algorithm to consider two species instead of one and to incorporate competitive kinetics instead of zero logistic source terms. This implementation is notably powerful and can be easily generalized to to enhance the understanding of the multiple swimming competing species responding to various chemical stimuli. , the directed movement of organisms in response to chemical gradients, is crucial in vari-

ous biological processes like embryogenesis, immunology, cancer growth and wound healing. It allows organisms to find nutrients, avoid predators or locate mates. For instance, cellular slime molds move towards higher chemical concentrations secreted by amoebae, while bacteria swim towards areas with more oxygen. In pancreatic cancer therapy, iodine acts as a chemoattractant to destroy cancer cells.

2 Setting of the problem

The assumptions given in this section, ensure that our model remains biologically realistic and mathematically well-posed. We suppose initially that $\chi_1(0) = \chi_2(0) = 0$ and that the chemotactic sensitivities χ_1 and χ_2 vanish when $M \geq 1$ and $W \geq 1$. This threshold condition, needed to prevent overcrowding, has a clear biological interpretation called the volume-filling effect (see [15]). The main assumptions are as follows:

$$\text{The functions } a,\ b,\ \chi_1,\ \chi_2 \text{ belong to the set} \tag{5}$$

$$\{w \in C([0,1],\mathbb{R}^+) \text{ such that } w(0) = w(1) = 0\}\,.$$

The potential function $\phi = \phi(x)$ satisfies

$$\nabla\phi \in (L^\infty(\Omega))^d\,. \tag{6}$$

The permeabilities Q, R and S in $\mathcal{M}_d(\mathbb{R})$ are symmetric and verify:

$$Q_{i,j}, R_{i,j} \text{ and } S_{i,j} \in L^\infty(\Omega),\ \forall i,j\,, \tag{7}$$

and there exist $c_Q \in \mathbb{R}_+^*$, $c_R \in \mathbb{R}_+^*$ and $c_S \in \mathbb{R}_+^*$ such that a.e. $x \in \Omega, \forall \xi \in \mathbb{R}^d$,

$$Q(x)\xi\cdot\xi \geq c_Q|\xi|^2,\ R(x)\xi\cdot\xi \geq c_R|\xi|^2 \tag{8}$$

and $S(x)\xi\cdot\xi \geq c_S|\xi|^2$.

Next, we require that there exist $\overline{D}$, $\overline{D_1} \in \mathbb{R}_+^*$ such that a.e. $x \in \Omega$, $\forall M \in [0,1]$,

$$||D(x,M)||_{\mathcal{M}_d(\mathbb{R})} = ||Q(x)a(M)||_{\mathcal{M}_d(\mathbb{R})} \leq \overline{D}\,, \tag{9}$$

$$||D_1(x,M)||_{\mathcal{M}_d(\mathbb{R})} = ||Q(x)\chi_1(M)||_{\mathcal{M}_d(\mathbb{R})} \leq \overline{D_1}\,.$$

and there exist $\overline{E}$ and $\overline{E_1} \in \mathbb{R}_+^*$ such that a.e. $x \in \Omega$, $\forall W \in [0,1]$,

$$||E(x,W)||_{\mathcal{M}_d(\mathbb{R})} = ||R(x)b(W)||_{\mathcal{M}_d(\mathbb{R})} \leq \overline{E}\,, \tag{10}$$

$$||E_1(x,W)||_{\mathcal{M}_d(\mathbb{R})} = ||R(x)\chi_2(W)||_{\mathcal{M}_d(\mathbb{R})} \leq \overline{E_1}\,.$$

Furthermore, the initial conditions are bounded as follows:

$$0 \leq M_0 \leq 1,\ 0 \leq W_0 \leq 1, C_0 \geq 0 \text{ a.e. in } \Omega \tag{11}$$

$$\text{and } C_0 \in L^\infty(\Omega)\,.$$

Finally, we introduce basic notations associated to the Navier-Stokes equation,

$$U_0 \in H \text{ and } g \in L^2(0,T;V') \text{ such that} \tag{12}$$

$$\wp = \{U \in \mathcal{D}(\Omega), \nabla\cdot U = 0\},\ V = \bar{\wp}^{H_0^1(\Omega)}$$

$$\text{and } H = \bar{\wp}^{L^2(\Omega)}\,.$$

Moreover, the form

$$\mathcal{B}(U,V_1,V_2) = \int_\Omega (U\cdot\nabla V_1)V_2\,dx \text{ is continuous} \tag{13}$$

$$\text{over } H_0^1(\Omega)\times H^1(\Omega)\times H^1(\Omega);\ \mathcal{B}(U,V,V) = 0\,.$$

Definition 2.1. *A quadruple* (M,W,C,U) *is called a* **weak solution** *of* (2) *if*

$$0 \leq M(x,t) \leq 1,\ 0 \leq W(x,t) \leq 1,\ C(x,t) \geq 0$$

$$M, W \in C_w(0,T;L^2(\Omega)),$$

$$\partial_t M, \partial_t W \in L^2(0,T;(H^1(\Omega))'),$$

$$A(M) := \int_0^M a(r)dr,\ B(W) \in L^2(0,T;H^1(\Omega))\,,$$

$$C \in L^\infty(Q_T)\cap L^2(0,T;H^1(\Omega))\cap C(0,T;L^2(\Omega));$$

$$U \in L^\infty(0,T;H)\cap L^2(0,T;V)\cap C_w(0,T;H);$$

$$\partial_t C \in L^2(0,T;(H^1(\Omega))'),\ \frac{dU}{dt} \in L^1(0,T;V'),$$

and (M,W,C,U) *satisfy*

$$\int_0^T < \partial_t M, \psi_1 >_{(H^1)',H^1} dt \tag{14}$$

$$+\iint_{Q_T} [Q(x)(a(M)\nabla M - \chi_1(M)\nabla C)]\cdot\nabla\psi_1\,dxdt$$

$$-\iint_{Q_T} MU\cdot\nabla\psi_1\,dxdt$$

$$= \mu_1\iint_{Q_T} M(1-M-\alpha_1 W)\psi_1\,dxdt\,,$$

$$\int_0^T < \partial_t W, \psi_2 >_{(H^1)',H^1} dt \tag{15}$$

$$+\iint_{Q_T} [R(x)(b(W)\nabla W - \chi_2(W))\nabla C]\cdot\nabla\psi_2\,dxdt$$

$$-\iint_{Q_T} WU\cdot\nabla\psi_2\,dxdt$$
$$=\mu_2\iint_{Q_T} W(1-W-\alpha_2 M)\psi_2\,dxdt\,,$$
$$\int_0^T <\partial_t C,\psi_3>_{(H^1)',H^1} dt \qquad (16)$$
$$+\iint_{Q_T} S(x)\nabla C\cdot\nabla\psi_3\,dxdt-\iint_{Q_T} CU\cdot\nabla\psi_3\,dxdt$$
$$=-\iint_{Q_T}(\alpha M+\beta W)C\psi_3\,dxdt\,,$$
$$\int_0^T <\partial_t U,\psi>_{V',V} dt \qquad (17)$$
$$+\nu\iint_{Q_T}\nabla U\cdot\nabla\psi\,dxdt+\kappa\iint_{Q_T}(U\cdot\nabla)U\,\psi\,dxdt$$
$$=-\iint_{Q_T}(\gamma M+\lambda W)\nabla\Phi\,\psi\,dxdt\,,$$

for all ψ_1, ψ_2, $\psi_3\in L^2(0,T;H^1(\Omega))$ *and* $\psi\in C_c^0(]0,T[;V)$,

where $C_c^0(]0,T[;V)$ denotes the space of continuous functions with compact support and $C_w(0,T;L^2(\Omega))$ denotes the continuous functions onto $L^2(\Omega)$ endowed with the weak topology.

Theorem 2.2. *Given assumptions* (5)-(13)*, the system* (2) *is* ***globally well-posed*** *in spatial dimensions* $d\leq 4$.

Indeed, the presence of singular degenerate diffusive terms can present challenges, such as limited regularity properties and difficulties in establishing uniform bounds of solutions. For that, a semi-discretization in time technique was used to construct an approximate solution for the non-degenerate problem. Then, we obtain a weak solution of the degenerate problem through tending the regularization parameter to zero. Moreover and for this system coupled with Stokes equations that assume negligible inertial forces, the uniqueness of weak solutions is well guaranteed under further conditions on the regularity of the initial data.

Next, this paper aims to combine the rigorous theoretical Theorem with the comprehensive numerical study of system (2). The validation of the theoretical results through the numerical analysis provides a robust framework for understanding the dynamics of competitive species influenced by anisotropy, chemotactic sensitivities, and fluids. The accuracy and the reliability of our model enhance its predictive capabilities for real-world biological systems.

3 Numerical combined FV-FE Scheme

This section is dedicated to formulating a combined scheme for the competitive two-species chemotaxis model (2) in fluid environments. The finite volume (FV) techniques impose restrictions on mesh structures, making them less flexible for complex geometries. On the other hand, the finite element (FE) methods often face instabilities, particularly in convection-dominated cases. Moreover, some FE numerical studies relates the accuracy of their solutions with the quality of the mesh, implying a significant limitation. This gap highlights the need for more robust numerical methods that can handle anisotropic diffusion, mesh flexibility, extension of one-species models, competitive Lotka-Volterra interactions and robustness in convection-dominated case. Consequently, recent numerical studies have explored a robust FV-FE scheme for parabolic equations in [16], for anisotropic Keller-Segel models in [17], and for one-species, anisotropic Keller-Segel-fluid model without logistic sources in [18]. In this paper, we extend this combined scheme: finite volumes and nonconforming finite elements, for a two-species chemotaxis-fluid model (2) incorporating Lotka-Volterra competition. First, we start by describing the space and time discretization and by defining the needed approximation spaces.

3.1 Space and Time Discretizations

We consider a family $\mathcal{T}_h$ of meshes of the domain Ω, consisting of disjoint closed simplices. The size of the mesh $\mathcal{T}_h$ is defined by $h:=\max_{K\in\mathcal{T}_h} diam(K)$. Then, we construct a dual partition $\mathcal{D}_h$ of diamonds, called control volumes of Ω such that $\bar{\Omega}=\cup_{D\in\mathcal{D}_h}\bar{D}$. Indeed, a unique diamond D is associated to each each side $\sigma_D=\sigma_{K,L}$ of the initial mesh. We construct it by connecting the barycenters of every $K\in\mathcal{T}_h$ that contains σ_D through the vertices of σ_D. The point P_D is referred to as the barycenter of the side σ_D. For all $D\in\mathcal{D}_h$, denote by $|D|$ the measure of D, by $\mathcal{N}(D)$ the set of neighbors of the volume D, by $\sigma_{D,E}$ the interface between a dual volume D and E and by $\eta_{D,E}$ the unit normal vector to $\sigma_{D,E}$ outward to D (see Fig. 1).

A discretization of $[0,T]$ is given by $\tilde{N}\in\mathbb{N}^*$ such that $t_n=n\tau$, for $n\in\{0,....,\tilde{N}\}$ and a constant step τ. The discrete unknowns are denoted by $\left\{w_D^n,\,D\in\mathcal{D}_h\right\}_{n\in\{0,...,,\tilde{N}\}}$ where $w=M$, W, C or U.

On the other hand, the approximate spaces are

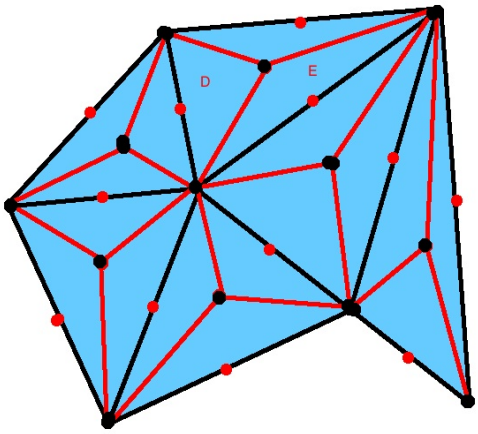

Figure 1: Primal and dual meshes.

defined as:

$$X_h := \{\varphi_h \in L^2(\Omega);\ \varphi_h|_K \text{ is linear } \forall K \in \mathcal{T}_h, \quad (18)$$
$$\varphi_h \text{ is continuous at the points } P_D,\ D \in \mathcal{D}_h^{int}\},$$
$$X_h^0 := \{\varphi_h \in X_h;\ \varphi_h(P_D) = 0,\ \forall D \in \mathcal{D}_h^{ext}\}.$$

The basis of X_h is spanned by the shape functions φ_D such that $\varphi_D(P_E) = \delta_{DE}$, $E \in \mathcal{D}_h$, δ being the Kronecker delta. The semi-norm $||M_h||_{X_h}^2 := \sum_{K\in\mathcal{T}_h} \int_K |\nabla M_h|^2 dx$ becomes a norm on X_h^0.

3.2 Numerical algorithm

Due to the incompressibility condition $\nabla \cdot U = 0$ and to approximate the space V defined in (12), even for Stokes equations, is very challenging. The simple finite elements, related to the dimension d of the space are very weak, since there is no basis for the approximate space V_h. Hence, we approach the fluid equations using nonconforming finite element methods to avoid all constraints.

Let us denote the approximation of the flux $Q(x)\nabla C \cdot \eta_{D,E}$ (resp. $U \cdot \eta_{D,E}$) on the interface $\sigma_{D,E}$ by $\delta C_{D,E}$ (resp. $U_{D,E}$). Then, to approximate the numerical flux $Q(x)\chi_1(M)\nabla C \cdot \eta_{D,E}$, we use the values M_D, M_E and $\delta C_{D,E}$ through a numerical flux function $G(M_D, M_E, \delta C_{D,E})$ satisfying stability and consistency properties. Similarly, we approximate the flux $MU \cdot \eta_{D,E}$ as an upwind convection function $G_1(M_D, M_E, U_{D,E}) = U_{D,E}^+ N_D - U_{D,E}^- N_E$, where $U_{D,E}^+$ and $U_{D,E}^-$ denote the positive and negative parts of $U_{D,E}$, respectively. Moreover, for all $M_h = \sum_{D\in\mathcal{D}_h} M_D\varphi_D \in X_h$, we define a discrete function of $A(M_h)$ as $A_h(M_h) = \sum_{D\in\mathcal{D}_h} A(M_D)\varphi_D$.

We are able now to explain the procedure for solving numerically the system (2). Given the solution $(\tilde{M}_h^n, \tilde{W}_h^n, \tilde{C}_h^n, U_h^n, P_h^n)$ at time t_n, we first calculate (U_h^{n+1}, P_h^{n+1}), at time t_{n+1}, through discretized fluid equations. Then, a Newton algorithm is implemented to compute the solution $(\tilde{M}_h^{n+1}, \tilde{W}_h^{n+1}, \tilde{C}_h^{n+1})$ of the nonlinear chemotaxis competitive system coupled with a bigradient method to solve linear systems arising from the Newton process. Below is the detailed iterative algorithm used in our approach.

First step: (Computation of U_h^{n+1} and P_h^{n+1}) The Navier-Stokes equations are interpreted as a variational problem with linear constraints. Given $\tilde{M}_h^n = \{M_D^n\}_{D\in\mathcal{D}_h}$, $\tilde{W}_h^n = \{W_D^n\}_{D\in\mathcal{D}_h}$, U_h^n and P_h^n at time t_n:

We compute $U_h^{n+1} \in X_h$ and $P_h^{n+1} \in Y_h$ as the limits of the sequences $(U_h^{n+1,r})_{r=0}^{+\infty}$ and $(P_h^{n+1,r})_{r=0}^{+\infty}$ using a classical Uzawa's algorithm.

Second step: Consider U_h^{n+1} from the first step and the initial variables,

$$M_D^0 = \frac{1}{|D|}\int_D M_0(x)\,dx,\ W_D^0 = \frac{1}{|D|}\int_D W_0(x)\,dx, \quad (19)$$
$$C_D^0 = \frac{1}{|D|}\int_D C_0(x)\,dx, \forall D \in D_h.$$

Then, for all $n \in \{0, 1, ..., \tilde{N}\}$, the following updates are performed through the following combined discrete scheme:

$$|D|\frac{M_D^{n+1} - M_D^n}{\Delta t} - \sum_{E\in\mathcal{D}_h} \mathcal{Q}_{D,E} A(M_E^{n+1}) \quad (20)$$
$$+ \sum_{E\in\mathcal{N}(D)} G(M_D^{n+1}, M_E^{n+1}; \delta C_{D,E}^{n+1})$$
$$+ \sum_{E\in\mathcal{N}(D)} G_1(M_D^{n+1}, M_E^{n+1}; U_{D,E}^{n+1})$$
$$= \mu_1 M_D^{n+1}(1 - M_D^{n+1} - \alpha_1 W_D),$$

$$|D|\frac{W_D^{n+1} - W_D^n}{\Delta t} - \sum_{E\in\mathcal{D}_h} \mathcal{R}_{D,E} B(W_E^{n+1}) \quad (21)$$

$$+ \sum_{E\in\mathcal{N}(D)} G(W_D^{n+1}, W_E^{n+1}; \delta C_{D,E}^{n+1})$$
$$+ \sum_{E\in\mathcal{N}(D)} G_1(W_D^{n+1}, W_E^{n+1}; U_{D,E}^{n+1})$$
$$= \mu_2 W_D^{n+1}(1 - W_D^{n+1} - \alpha_2 M_D^n)\,,$$

$$|D|\frac{C_D^{n+1} - C_D^n}{\Delta t} - \sum_{E\in\mathcal{D}_h} \mathcal{S}_{D,E} C_E^{n+1} \qquad (22)$$
$$+ \sum_{E\in\mathcal{N}(D)} G_1(C_D^{n+1}, C_E^{n+1}; U_{D,E}^{n+1})$$
$$= -(\alpha M_D^{n+1} + \beta W_D^{n+1}) C_D^{n+1}\,.$$

The new transmissibilities

$$\mathcal{Q}_{D,E} = -\sum_{K\in\mathcal{T}_h} (\mathcal{Q}(x)\nabla\varphi_E, \nabla\varphi_D)_{0,K}\,,$$

for each pair of diamonds D and $E \in \mathcal{D}_h$, are the elements of the stiffness matrix of the nonconforming finite element method. Hence, the discrete diffusive fluxes are proved to be conservative, coercive and continuous. Additionally, the transmissibilities are bounded.

Remark 3.1. *To maintain the discrete maximum principle, we assume that all transmissibilities are positive. If not, one can use a nonlinear technique inspired by [19] to correct the diffusive flux blocking the discrete maximum principle and to maintain the monotonicity and the convergence of the corrected numerical scheme.*

3.3 Convergence of the numerical scheme

To ensure the reliability and accuracy of our combined scheme, we investigate the convergence properties of the numerical solutions. We define two types of approximate solutions: A finite volume solution $\left(\tilde{M}_{h,\Delta t}(x,t),\, \tilde{W}_{h,\Delta t}(x,t),\, \tilde{C}_{h,\Delta t}(x,t)\right) = \left(M_D^{n+1},\, W_D^{n+1},\, C_D^{n+1}\right)$ defined as piecewise constant on the dual volumes D in space and piecewise constant in time (**represented by the red points in Figure 1**) and a nonconforming finite element solution ($M_{h,\Delta t}$, $W_{h,\Delta t}$, $C_{h,\Delta t}$) as a piecewise linear and continuous in the barycenters of the interior sides in space and piecewise constant in time (**represented by the black points of Figure 1**). Again, the numerical solutions are bounded and hence biologically admissible. Indeed, $\forall D \in \mathcal{D}_h$, $k \in \{0, 1, ..., \tilde{N}\}$,

$$0 \le M_D^k \le 1, 0 \le W_D^k \le 1 \text{ and } 0 \le C_D^k \le \zeta\,.$$

Furthermore, if $U_0 \in L^\infty(\Omega)$ then

$$||U_0||_{L^\infty(\Omega)} - (T+1)||\nabla\phi||_{L^\infty(\Omega)} \le U_h^k$$
$$\le ||U_0||_{L^\infty(\Omega)} + (T+1)||\nabla\phi||_{L^\infty(\Omega)},$$

for all $k \in \{0, ..., \tilde{N}\}$ and $k\tau \le T$. We now state the main convergence Theorem for the discrete Navier-Stokes equation, extended from [[20], ch. VII, Proposition 6.7].

Theorem 3.2. *(**Convergence of the discrete NS equations**) Assume* (12)-(13)*, then:*
a) There exists a unique discrete solution $U_{h,\Delta t}$ if $d = 2$ and there exists at least one such solution if $d \le 4$.
b) As h and Δt tend to zero, and modulo subsequences:
$U_{h,\Delta t} \to U \in L^2(Q_T)$ strongly and $U_{h,\Delta t} \overset{*}{\rightharpoonup} U$ in $L^\infty(0,T;L^2(\Omega))$.

Theorem 3.3. *(**Convergence of the combined scheme**)*
1) There exists a solution $(\tilde{M}_{h,\Delta t}, \tilde{W}_{h,\Delta t}, \tilde{C}_{h,\Delta t})$ of the discrete system (20)-(22) *with initial data* (19).
2) Any sequence $(h_m)_m$ decreasing to zero possesses a subsequence such that $(M_{h_m}, W_{h_m}, C_{h_m}, U_{h_m})$ converges a.e. on Q_T to a solution (M, W, C, U) of the chemotaxis-fluid system (2) *in the sense of Definition 2.1 .*

For the discrete two-species chemotaxis model, many estimates for system (2) remain true due to the discrete maximum principle well-satisfied and to the boundedness of all logistic sources in L^∞. Using the same guidelines of the discrete one-species chemotaxis model, the existence of discrete solutions and the convergence towards a weak solution of the continuous problem are well proved.

4 Numerical Simulations

Numerical discrete solutions are presented in this section to validate the theoretical approach, to handle complex anisotropic two-species models in fluids and to understand the complex competitive dynamics of the living organisms. An extended Fortran code implements the combined scheme

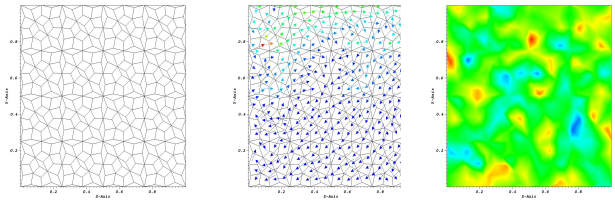

Figure 2: Dual Mesh, fluid flow and random initial densities of species .

and hence it is adaptable to various mesh configurations and to general parameter settings. The simulations aim to answer how current-related organisms affect competition and survival rates, explore defense strategies over time and determine critical thresholds where significant changes in populations occur in response to variations in model parameters.

To reflect the habitat heterogeneity and the diffusion anisotropy of species, we consider the full system (2) with corresponding diffusive and convective coefficients. The simulations are performed on the mesh given in Figure 2, with random initial conditions for species densities $M_0(x, y)$ and $W_0(x, y)$ between 0 and 1. Moreover, the initial chemical concentration $C_0(x, y) = 1$ is defined by regions. The fluid flow surrounding the species is given as a driven cavity (see Figure 2) which is created by a zero initial velocity vector with a constant speed $(1, 0)$ on the top wall of the domain. Then, the following parameters are used: the time step $dt = 0.0005$ along with the model parameters $\alpha = 0.06$, $\beta = 0.08$, $\gamma = 0.01$, $\lambda = 0.01$, $c_1 = 0.001$, $c_2 = 0.001$, $c_3 = 0$, $\tilde{D}_1 = 0.001$, $c_4 = 0.1$, $\tilde{D}_2 = 0.001$, $c_5 = 0.1$, $\tilde{D}_3 = 10^{-5}$, $\nu = 0.001$, $\kappa = 1$ and $\nabla\phi = (0.1, 0.1)$. Additionally, the logistic growth rates are $\mu_1 = \mu_2 = 1$ and the competition coefficients are $\alpha_1 = 4 > 1 > \alpha_2 = 0.01$. Next, distinctive heterogeneous and anisotropic tensors are chosen: species 1 uses a homogeneous anisotropic tensor $Q = \begin{bmatrix} 8 & -7 \\ -7 & 20 \end{bmatrix}$, whereas species 2 employs a heterogeneous rotational anisotropic tensor $R(x, y) = \frac{1}{x^2+y^2}\begin{bmatrix} y^2+0.01x^2 & -(1-0.01)xy \\ -(1-0.01)xy & x^2+0.01y^2 \end{bmatrix}$. Figure 3 illustrate the behavior of the species within the fluid environment over time. The simulations demonstrate that the species 2 exhibits a faster victory in competition compared to species 1 after 20 seconds.

Otherwise, to simulate the collaboration between species to avoid chemicals, a second test has been given with $\alpha_1 = \alpha_2 = 0.1 < 1$ within an oblique fluid flow. In this case, the tensors are chosen to be $Q = R = \begin{bmatrix} 8 & -7 \\ -7 & 20 \end{bmatrix}$. The evolution of the variables is given in Figure 4. To sum up, these numerical results align with the theoretical coexistence or extinction of species, related to the values of α_i; $i = 1, 2$ and with the survival behavior of living organisms in fluid environments.

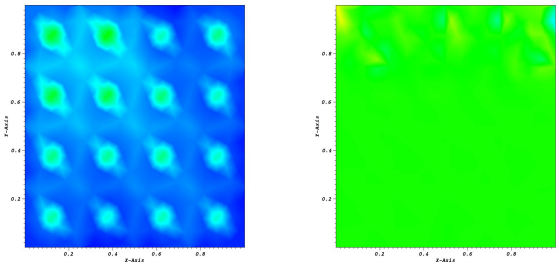

Figure 3: Density of species 1 after 20 s ; $10^{-23} \leq M \leq 10^{-11}$ (left). Density of species 2 after 20 s; $0.994 \leq W \leq 0.999$ (right).

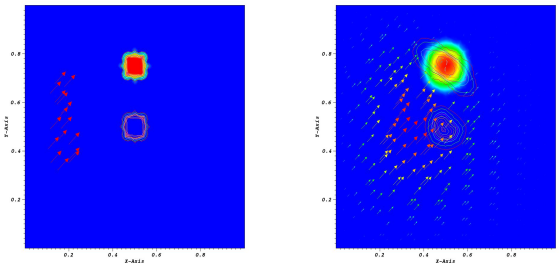

Figure 4: Coexistence case: avoiding enemies and predators. .

5 Conclusion

The combination of theoretical insights and computational simulations in this work offers a comprehensive understanding of the dynamics involving anisotropic species interactions in fluid environments. The global existence of weak solutions is the first theoretical contribution due to regularization techniques and suitable estimates. The second main contribution is the numerical analysis of the model. This includes addressing the specific challenges of different possible scenarios in [21]. Finally, a series of numerical tests are conducted to reveal a range of outcomes from stable coexistence to competitive exclusion. As a perspective to this work, all the numerical data may be collected to train computers and can be en-

hanced with artificial intelligence techniques to calibrate the model parameters to reduce the loss error between the numerical and the real data. Moreover, this mathematical study may be applied to haptotaxis-fluid models and hence to a deeper and a predictive analysis of the cancer tumor growth models.

References:

[1] A. J. Lotka, *Elements of physical biology.* Williams and Wilkins, 1925.

[2] V. Volterra, *Variations and fluctuations of the number of individuals in animal species living together.* ICES Journal of Marine Science, Vol. 3, No. 1, 1928, pp. 3-51.

[3] Y. Lou and W.-M. Ni, *Diffusion vs cross-diffusion: an elliptic approach.* J. Differential Equations, Vol. 154, No. 1, 1999, pp. 157-190.

[4] M. Mimura and K. Kawasaki, *Spatial segregation in competitive interaction-diffusion equations.* J. Math. Biol., Vol. 9, No. 1, 1980, pp. 49-64.

[5] E. F. Keller and L. A. Segel, *Model for chemotaxis.* Journal of theoretical biology, Vol. 30, No. 2, 1971, pp. 225-234.

[6] D. Horstmann, *From 1970 until present: the Keller-Segel model in chemotaxis and its consequences. I.* Jahresber. Deutsch. Math.-Verein., Vol. 105, No. 3, 2003, pp. 103-165.

[7] G. Chamoun, *Mathematical analysis of parabolic models with volume-filling effect in weighted networks.* Journal of Dynamics and Differential Equations, Vol. 35, No. 3, 2023, pp. 2115-2137.

[8] J. I. Tello and D. Wrzosek, *Predator-prey model with diffusion and indirect prey-taxis.* Mathematical Models and Methods in Applied Sciences, Vol. 26, No. 11, 2016, pp. 2129-2162.

[9] M. Bendahmane and M. Langlais, *A reaction-diffusion system with cross-diffusion modeling the spread of an epidemic disease.* Journal of Evolution Equations, Vol. 10, No. 4, 2010, pp. 883-904.

[10] H-Y. Jin and T. Xang, *Convergence rates of solutions for a two-species chemotaxis-Navier-Stokes system with competitive kinetics* Discrete and continuous dynamical systems-B, Vol. 24, No. 4, 2019, pp. 1919-1942.

[11] C. Stinner, J.I. Tello and M. Winkler, *Competitive exclusion in a two-species chemotaxis model* J. Math Biol. , Vol. 68, No. 7, 2014, pp. 1607-1626.

[12] M. Hirata, S. Kurima, M. Mizukami and T. Yokota *Boundedness and stabilization in a three-dimensional two-species chemotaxis-Navier-Stokes system* Proceedings of Equadiff 2017 Conference, Bratislava, July 24-28, 2017, pp. 11-20.

[13] X. Cao, S. Kurima and M. Mizukami, *Global existence and asymptotic behavior of classical solutions for a 3D two-species chemotaxis-Stokes system with competitive kinetics* Math Meth Appl Sci., Vol. 41, 2018, pp. 3138-3154.

[14] G. Li and Y. Yao, *Two-species competition model with chemotaxis: well-posedness, stability and dynamics.* Nonlinearity, Vol 35, No. 3, 2022, pp. 1329-1359.

[15] T. Hillen and K. Painter, *Volume filling effect and quorum-sensing in models for chemosensitive movement.* Canadian App. Math., Vol. 10, 2002, pp. 501-543.

[16] R. Eymard, D. Hilhorst and M. Vohralik, *A combined finite volume-nonconforming/mixed hybrid finite element scheme for degenerate parabolic problems.* Numer. Math., Vol. 105, 2006, pp. 73-131.

[17] R. Eymard, D. Hilhorst and M. Vohralik, *A combined finite volume-nonconforming/mixed hybrid finite element scheme for degenerate parabolic problems.* Numer. Math., Vol. 105, 2006, pp. 73-131.

[18] A. Lorz, *A coupled KellerSegelStokes model: Global existence for small initial data and blow-up delay.* COMMUN. MATH. SCI, Vol. 10, No. 2, 2013, pp. 555-574.

[19] C. Cances, M. Cathala and C. Le Poitier, *Monotone corrections for generic cell-centered finite volume approximations of anisotropic diffusion equations.* Numer. Meth., Vol. 125, 2013, pp. 387-417.

[20] R. Temam, *Navier-Stokes Equations.* Edition AMS CHELSEA, 2000.

[21] J.D. Murray, *Mathematical Biology II.* Third Edition, Springer, 2001.

Contribution of Individual Authors to the Creation of a Scientific Article (Ghostwriting Policy)

The author contributed in the present research, at all stages from the formulation of the problem to the final findings and solution.

Sources of Funding for Research Presented in a Scientific Article or Scientific Article Itself

No funding was received for conducting this study.

Conflicts of Interest

The author has no conflicts of interest to declare.